RESEARCH ARTICLE | *Control of Movement*

Effects of mirror-box therapy on modulation of sensorimotor EEG oscillatory rhythms: a single-case longitudinal study

Roman Rosipal,[1,3] Natália Porubcová,[1] Peter Barančok,[2] Barbora Cimrová,[2] Igor Farkaš,[2] and Leonardo Jose Trejo[3]

[1]*Institute of Measurement Science, Slovak Academy of Sciences, Bratislava, Slovakia;* [2]*Faculty of Mathematics, Physics and Informatics, Comenius University in Bratislava, Bratislava, Slovakia; and* [3]*Pacific Development and Technology, LLC, Palo Alto, California*

Rosipal R, Porubcová N, Barančok P, Cimrová B, Farkaš I, Trejo LJ. Effects of mirror-box therapy on modulation of sensorimotor EEG oscillatory rhythms: a single-case longitudinal study. *J Neurophysiol* 121: 620–633, 2019. First published December 12, 2018; doi:10.1152/jn.00599.2018.—We provide direct electrophysiological evidence that mirror therapy (MT) can change brain activity and aid in the recovery of motor function after stroke. In this longitudinal single-case study, the subject was a 58-yr-old man with right-hand hemiplegia due to ischemic stroke. Over a 9-mo period we treated him with MT twice a week and measured electroencephalograms (EEG) before, during, and after each therapy session. Using advanced signal processing methods, we identified five distinct movement-related oscillatory EEG components: one slow component designated as mu rhythm and four faster components designated as sensorimotor rhythms. Results show that MT produced long-term changes of two oscillatory EEG components including the mu rhythm, which is a well-documented correlate of voluntary movement in the frequency range of 7.5–12 Hz. Specifically, MT was significantly associated with an increase in the power of mu rhythm recorded over both hemispheres and a decrease in the power of one sensorimotor component recorded over the affected hemisphere. To obtain robust, repeatable individual measures of EEG components suitable for longitudinal study, we used irregular-resampling autospectral analysis to separate fractal and oscillatory components in the EEG power spectrum and three-way parallel factor analysis to isolate oscillatory EEG components and track their activations over time. The rhythms were identified over individual days of MT training and were clearly related to the periods of event-related desynchronization and synchronization (rest, observe, and move) during MT. Our results are consistent with a model in which MT promotes recovery of motor function by altering neural activity associated with voluntary movement.

NEW & NOTEWORTHY We provide novel evidence that mirror therapy (MT), which helps in the recovery of motor function after a stroke, is also associated with long-lasting changes in brain electrical activity. Using precise measurements of oscillatory EEG components over a 9-mo period in a victim of ischemic stroke, we showed that MT produced long-term increases in the mu rhythm recorded over both hemispheres and a decrease in a sensorimotor EEG component recorded over the affected hemisphere.

biofeedback; EEG oscillatory rhythms; mirror therapy; neural plasticity; stroke

INTRODUCTION

Hemiparesis or hemiplegia of the upper limbs are one of the major motor impairment consequences of stroke. Current rehabilitation methods only help a fraction of stroke victims to recover. Even after months of intense rehabilitation efforts only ~50% of patients show motor impairments (Jones et al. 2011). Research efforts should focus on developing novel rehabilitation strategies, such as mirror therapy (MT), to improve the quality of life of patients after stroke and to reduce their dependence on others.

MT is a visual feedback training procedure in which an individual rehearses a limb movement by reflected movements of the nonparetic side in a mirror as if it were the affected side. In healthy subjects, mirror visual feedback can increase action-related motor competence in an untrained hand (Bähr et al. 2018). In stroke patients, randomized prospective trials of MT have shown that although some recovery occurred with sham treatments, MT led to significantly greater recovery of upper extremity function (Gurbuz et al. 2016; Lim et al. 2016). A meta-analysis of 15 studies of MT for upper extremity rehabilitation in stroke patients concluded that MT alone provided better results in promoting recovery than conventional rehabilitation alone or combined with MT (Pérez-Cruzado et al. 2017).

The physiological basis of mirror therapy effectiveness stems from the existence of neural pathways by which primary cortex excitability is modulated by passive visual observation of contralateral limb movement as well as by voluntary movement of the ipsilateral limb. Using transcranial magnetic stimuli to induce motor evoked potentials, Garry et al. (2005) found that excitability of primary motor cortex ipsilateral to a unilateral hand movement was modulated by viewing a mirror image of the active hand. EEG rhythms, such as mu rhythm, reflect unilateral activations of motor cortex associated with voluntary real or imagined movement, by suppressing the rhythm arising from contralateral motor cortex. This suppression also occurs when viewing images of their movements or even movements

performed by others. The suppression effects arising from viewing limb motions may arise from the ventral premotor cortex (Oberman et al. 2007; Pineda 2005), which in primates has strong corticocortical connections with the motor cortex (Shimazu et al. 2004).

The clear relationship between the effects of mirror visual feedback of limb movement and mu rhythm suppression, as well as the evidence for modulation of motor cortex by the mirror neuron system, leads to the hypothesis that we may objectively estimate and track MT effectiveness over time by measuring associated changes in motor-related EEG rhythms. EEG recorded from the scalp originates from electrical currents generated by a mixture of a large number of quasirandom neural sources across the entire cortex (broadband background EEG) and a small number of more localized cortical sources whose power spectra are narrow band (oscillatory) such as the well-known alpha rhythm, sensorimotor rhythms, and some beta rhythms (He 2014; Nunez and Srinivasan 2006). A subset of these oscillatory rhythms closely reflects movement-related activity during the preparation, execution, and postmovement periods (Pfurtscheller and Lopes da Silva 1999; Pineda 2005). Narrow-band oscillatory rhythms associated with movement and with cortical sources in the sensorimotor cortical areas are found in the range of frequencies from 7 to 30 Hz (Pfurtscheller and Lopes da Silva 1999).

Decreases or increases of EEG power of movement-related oscillatory rhythms during movement represent the well-known phenomena of event-related desynchronization (ERD) or synchronization (ERS) (Pfurtscheller and Lopes da Silva 1999). Studies have shown that ERD/ERS can also be elicited by imagined movements without physical execution of the movement itself. Imaginary motion represents an important component of many brain-computer interface designs also targeted for neurorehabilitation purposes (Chaudhary et al. 2016). Behavioral and physiological correlates of imaginary motion and passive observation of real movements are similar, and both activities are associated with the mirror neuron system (Case at al. 2015; Mulder 2007; Rizzolatti and Craighero 2004). Therefore, ERD and ERS of movement-related EEG rhythms will occur with real or observed movements during training with a mirror box.

We do not yet know if mirror-box training can produce quantitative changes in the power spectrum of oscillatory rhythms or if such changes reflect the efficacy of MT. To answer this question, we compared the power spectra of motor-related oscillatory rhythms from resting EEG before and after mirror-box training. Unlike visual alpha blocking, movement-related oscillatory rhythms are suppressed by either real or imaginary movement but not by opening the eyes (Pineda 2005). This allows us to detect their synchronization pattern during both eyes-open and eyes-closed resting conditions. We studied short-term (session- or day-based) and long-term (across the 9-mo long intervention period) power spectrum changes. To our knowledge, this is the first longitudinal study focusing on an effect of MT on EEG oscillatory components. We do not have an a priori hypothesis about the direction of these changes. Therefore, the study is explanatory, supported by an adequate number of repeated measures and providing acceptable statistical power for the results.

Large interindividual differences of the central peak frequency and also spatial distribution of the EEG oscillatory rhythms exist (Doppelmayr et al. 1998; Klimesch 1996). Furthermore, the EEG frequency can vary as a function of experimental conditions or a subject's mental status. Therefore, to determine subject's individual EEG oscillatory rhythms, frequency and spatial information must be combined and, if possible, related to the expected changes determined by the experimental conditions. Conventional two-dimensional (2D) decomposition techniques [for example, principal component analysis (PCA) or independent component analysis (ICA)] are not ideally suited to reveal the existing latent data structure of EEG, because unfolding 2D decompositions can be done in several ways, and interactions of dimensions are not modeled well in 2D decompositions. For example, using either principal component analysis or independent component analysis for EEG source separation uses time-series and spatial information but ignores spectral information. Power spectra of extracted principal components or independent components must be estimated post hoc after the decomposition is performed, and the spectra of the sources do not constrain the solutions. 2D methods also suffer from nonuniqueness of the solution, and this needs to be overcome by imposing additional constrains on the extracted components such as orthogonality or independence.

To model the latent structure of multichannel EEG, multiway methods decompose the signals into a unique set of spectral, spatial, and temporal components. In this study, we used a three-way parallel factor analysis (PARAFAC) model to decompose EEG and identify unique space-time-frequency components or "atoms," representing narrow-band EEG oscillatory rhythms (Miwakeichi et al. 2004; Rosipal et al. 2009). Estimates of the power spectra and spatial distributions of each atom are given by corresponding vectors of loadings on the spectral or spatial dimensions. The vector of loadings on the time dimension or "time scores" represent the activation or deactivation of each atom over time and can be used to test the significance of changes over time or conditions. This effectively leads to the possibility of testing an EEG change, for example, the change in the power of a single oscillatory rhythm, through a single variable, thereby reducing a complex multidimensional signal to a scalar quantity. Our longer term experience with using PARAFAC in EEG decomposition shows that a set of stable EEG atoms can be extracted considering different experimental conditions and time points (Rosipal et al. 2009; Trejo et al. 2009). The stability of the PARAFAC decomposition of EEG was also confirmed recently by Mareček et al. (2017).

Because EEG consists of a mixture of signals from broadband background sources and a few more spatially focused oscillatory sources, it is important to "whiten" the EEG spectrum to separate background and oscillatory activity. Although many methods are applicable, the irregular-resampling autospectral analysis (IRASA) method provides a highly accurate and efficient solution for EEG spectral analysis (He 2014; Wen and Liu 2016). To study and test the changes of oscillatory rhythms at each EEG electrode separately, we used the IRASA method to separate fractal (representing background EEG) and harmonic (representing oscillatory EEG) components in the EEG power spectrum.

MATERIALS AND METHODS

Subjects

The subject of this longitudinal study was a 58-yr-old man who had a right-hand hemiplegia due to an ischemic stroke that had occurred to him 2 yr before he entered this study. He had no significant past medical history, and an MRI revealed ischemia extending from the fronto-temporal to parietal areas on the left side (Fig. 1). The subject received an explanation of the purpose and procedures of the study, which he fully understood, and gave written informed consent to participate. During the study he showed a normal level of consciousness, his language comprehension was intact, and he could communicate quite well despite mild dysarthria. His Mini-Mental State Examination (MMSE) score was 24 out of 30 (Pangman et. al. 2000). Neurological assessment before starting the study exhibited spastic hemiparesis on the right side, more seriously on the hand, which was plegic. He could walk quite well, and the superficial and deep sensation on the right side was normal. He underwent the assessment of the upper extremity: Fugl-Meyer Assessment (FMA), Modified Stroke Impact Scale (MSIS), and Modified Ashworth Scale (MAS), the measurement of the range of the volitional movements of upper extremity in his right shoulder and right elbow and forearm. The assessment was done every 6 wk between July 2014 and April 2015. During that period, the subject also participated in mirror therapy twice a week in addition to conventional rehabilitation, also twice a week.

Experimental Protocol

Our experimental paradigm of the MT was designed following the patient's actual level of performance and abilities of the execution of arm, hand, and finger postures (Fig. 2 illustrates the experimental protocol). Each training day (session) started with 2 min of the resting state block with eyes closed (EC) followed by 2 min of the resting state block with eyes open (EO). During the EO condition, the patient fixated his eyes on a small cross on the wall. The core part of MT consisted of two blocks of mirror box training. These blocks were followed by additional 2-min long resting periods of EO and EC. In each mirror box training block there were 12 different types of movement exercises. Each block started with a 30-s long EO resting period. Then a technician without motor disabilities, sitting opposite the patient, demonstrated three to four repetitions of a given movement type. After this demonstration, the patient started to execute a given movement self-paced from 7 to 10 times. Afterwards, the EO resting period followed for 10 s, before the technician demonstrated the next movement type. The whole procedure was repeated for all 12 movements. The training block ended with a 30-s long EO resting period. To keep track of the executed steps within the whole training block, the technician marked each step change by pressing a button on the keyboard. During the training, the patient sat comfortably behind a table with his affected arm hidden in the mirror box. During the first training block the patient moved his unaffected arm and watched its mirror image as if it were the affected one [visual left hand (VLH) block]. During the second block of movements, while still watching the movement of the unaffected arm in the mirror, the patient attempted to execute the same movement with his affected arm in the mirror box [visual both hands (VBH) block].

Data Acquisition

During all resting and mirror box training blocks a trained technician recorded EEG continuously using 12 active Ag/AgCl electrodes embedded in an elastic fabric cap (g.GAMMAcap; g.tec medical engineering, Schiedlberg, Austria). The technician placed the electrode cap on the participant's head according to the manufacturer's instructions, attaching six active EEG left-side scalp electrodes (FC3, C1, C3, C5, CP3, and O1), six active right-side electrodes (FC4, C2,
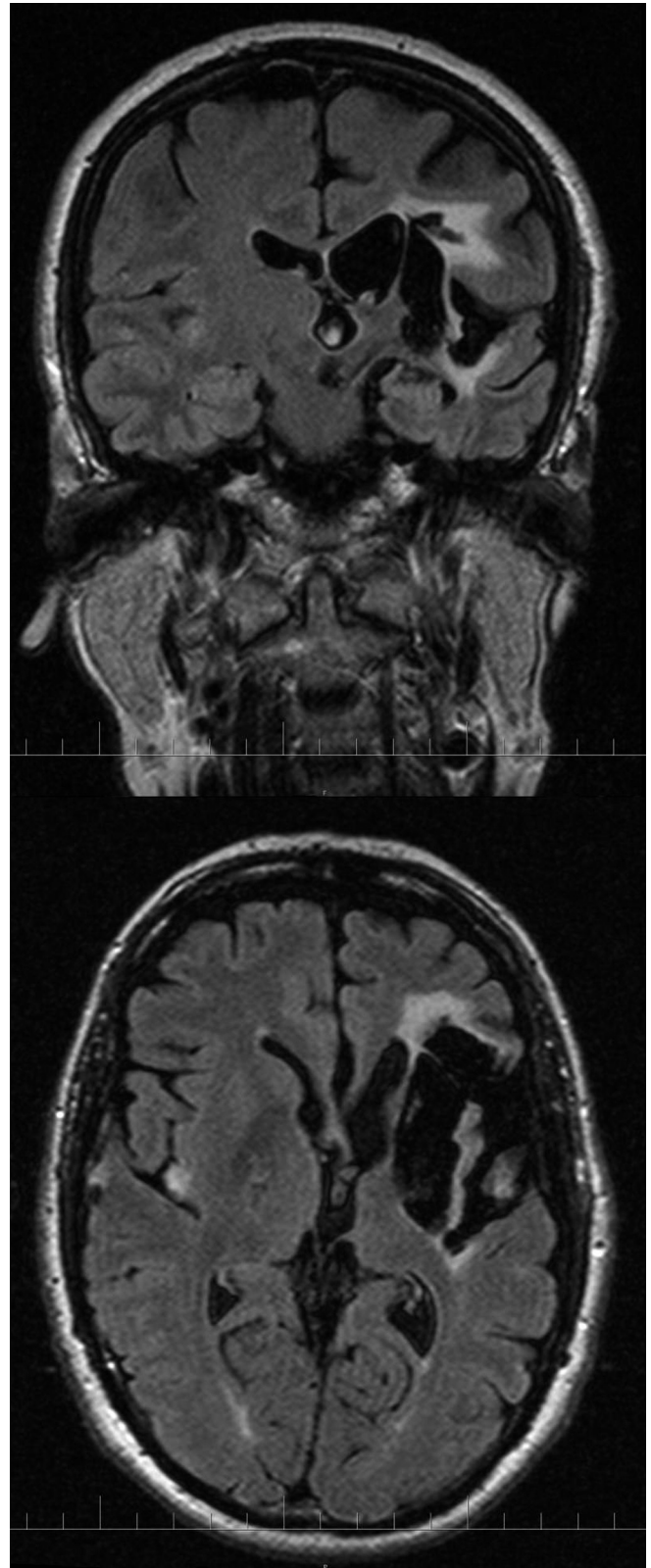

Fig. 1. Frontal and transversal, from the bottom of the head, MRI scan of the treated 58-yr-old man who had a right-hand hemiplegia due to an ischemic stroke.

C4, C6, CP4, and A2), one reference electrode (A1), and one ground electrode (AFz). Later, for signal processing we used the signal from the A2 electrode to re-reference all EEG recordings to the average earlobe [(A1 + A2)/2] signal. A 16-channel g.USBamp system (g.tec
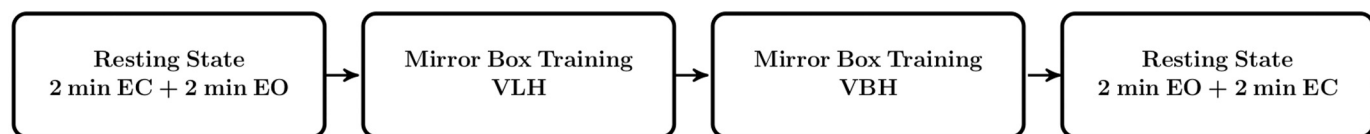
Fig. 2. *Top:* schema of the experimental protocol. Resting state blocks with eyes closed (EC) and eyes open (EO) are followed by the 2 mirror box training blocks that differ only in the instruction for the subject during the self-execution of a movement. The session is closed by repeating the resting state block. For details, see the text. *Bottom:* subject performing the mirror therapy training. VLH, visual left hand; VBH, visual both hands.

medical engineering), with the sampling rate of 512 Hz, band-pass 0.1–200 Hz, and notch filtering at 50 Hz, served to record all EEG signals. We digitized and stored all EEG signals on hard disk drives of a computer equipped with g.Recorder software (g.tec medical engineering) and archived all the data on a network-attached storage system.

EEG Data Analysis

We performed initial analyses using BrainVision Analyzer 2 software (BVA2; Brain Products). This involved the following steps: down sample signals to 128 Hz, apply automatic artifact detection with criteria of maximal allowed voltage step 50 μV/ms, lowest allowed activity in intervals of 100 ms set to 0.5 μV, and maximal allowed difference of voltages in intervals of 20 ms set to 50 μV. If any of the first two criteria were met, the interval preceding and following the detected artifact by 150 ms was marked as bad. It the case of the third criterion, this interval was set to ± 50 ms. Next, a

trained technician applied a careful manual inspection of the data and detected artifacts, also using the BVA2 software. The technician manually marked periods with undetected artifacts and removed artifact markers wrongly assigned automatically. This included detection and removal of ocular artifacts.

Next, we analyzed the EEG data using custom MATLAB scripts (The MathWorks). We first segmented EEG recordings into 2- or 4-s long overlapping segments (87.5% overlap) and zero-centered each segment by subtracting the mean segment voltage from each sample. We rejected any segment containing artifacts. After this procedure, for ~2-min-long resting state blocks, we retained, on average, 56 (94%) nonoverlapping 2-s segments and 26 (90%) 4-s segments. Segments of different lengths were analyzed as follows:

For the 2-s long segments, we used fast Fourier transforms with a Hanning window and the number of fast Fourier transforms points equal to the number of points in the segment to compute power spectrum densities (PSD) in the range of 0–64 Hz. We then analyzed

logarithmically transformed PSDs of segments with a three-way PARAFAC model (Bro 1997). PARAFAC is a generalization of PCA for dealing with multidimensional data. However, the uniqueness of the obtained decomposition gives the PARAFAC model an unsurpassed advantage over PCA (Bro 1997). Let us define a three-dimensional data matrix $\mathbf{X}$ ($I \times J \times K$) of PSD estimates at I time segments, J electrodes, and K frequencies. Then, three loading matrices, $\mathbf{A}$, $\mathbf{B}$, and $\mathbf{C}$ with elements $a_i^{(f)}$, $b_j^{(f)}$, and $c_k^{(f)}$ define the PARAFAC model that decomposes $\mathbf{X}$ and that can be mathematically described as

$$x_{ijk} = \sum_{f=1}^{F} a_i^{(f)} b_j^{(f)} c_k^{(f)} + \varepsilon_{ijk}$$

where x_{ijk} are elements of $\mathbf{X}$, ε_{ijk} are the residual errors, and F stands for a number of components (atoms) considered. The loadings elements are then found by minimizing the sum of squares of the residuals ε_{ijk} (Bro 1997), that is

$$\min_{a_i^{(f)} b_j^{(f)} c_k^{(f)}} \left\| x_{ijk} - \sum_{f=1}^{F} a_i^{(f)} b_j^{(f)} c_k^{(f)} \right\|^2$$

In our case, the PARAFAC loadings (weights) represent time, space, and frequency dimensions of the decomposition. For the PARAFAC analyses we used APECSgui, a set of proprietary MATLAB codes developed by Pacific Development and Technology (2012) and subroutines from the public N-way toolbox for MATLAB (Andersson and Bro 2000). The input consisted of sets of multichannel PSDs for each segment within an analysis period (e.g., pretraining EO) within the frequency range of 3.5–24.5 Hz. We also constrained the solution of PARAFAC to nonnegativity of the time scores and spatial weights and nonnegativity and unimodality of the frequency weights. The nonnegativity constraints disallow negative time, negative space, and negative frequency loadings, which facilitate physically plausible interpretations. The unimodality constrain serves to localize oscillatory components in the EEG spectrum to bands surrounding a true peak and disallows multiple peaks components with no spectral peak. This constraint serves to allow parsimonious physiological interpretations of EEG oscillations.

For the 4-s-long segments, we used the IRASA method to separate fractal and harmonic (oscillatory) components in the power spectrum of EEG segments according to their distinct temporal and spectral characteristics (Fig. 3; Wen and Liu 2016). For the decomposition, we used the IRASA toolbox for MATLAB freely available from the authors. We modified the code by setting possible negative spectral densities of the oscillatory part estimate to 0, used the Hanning window, and set the number of subsets for the PSD estimate to 10.

Statistical Analysis

We used two standard statistical approaches to determine significant short-term (day-based) and long-term (across intervention period) effects of the mirror box training. First, we used paired t-tests served to compare the differences of pre- and posttraining mean values of the investigated oscillatory EEG responses, factored by EC and EO conditions and by the spatial EEG electrodes placement factor. Second, we used a linear regression model served to test the longitudinal effects of the mirror box training over the whole experiment. In the model, the independent variable is represented by date and the dependent variable by the EEG response. The model can be schematically written as
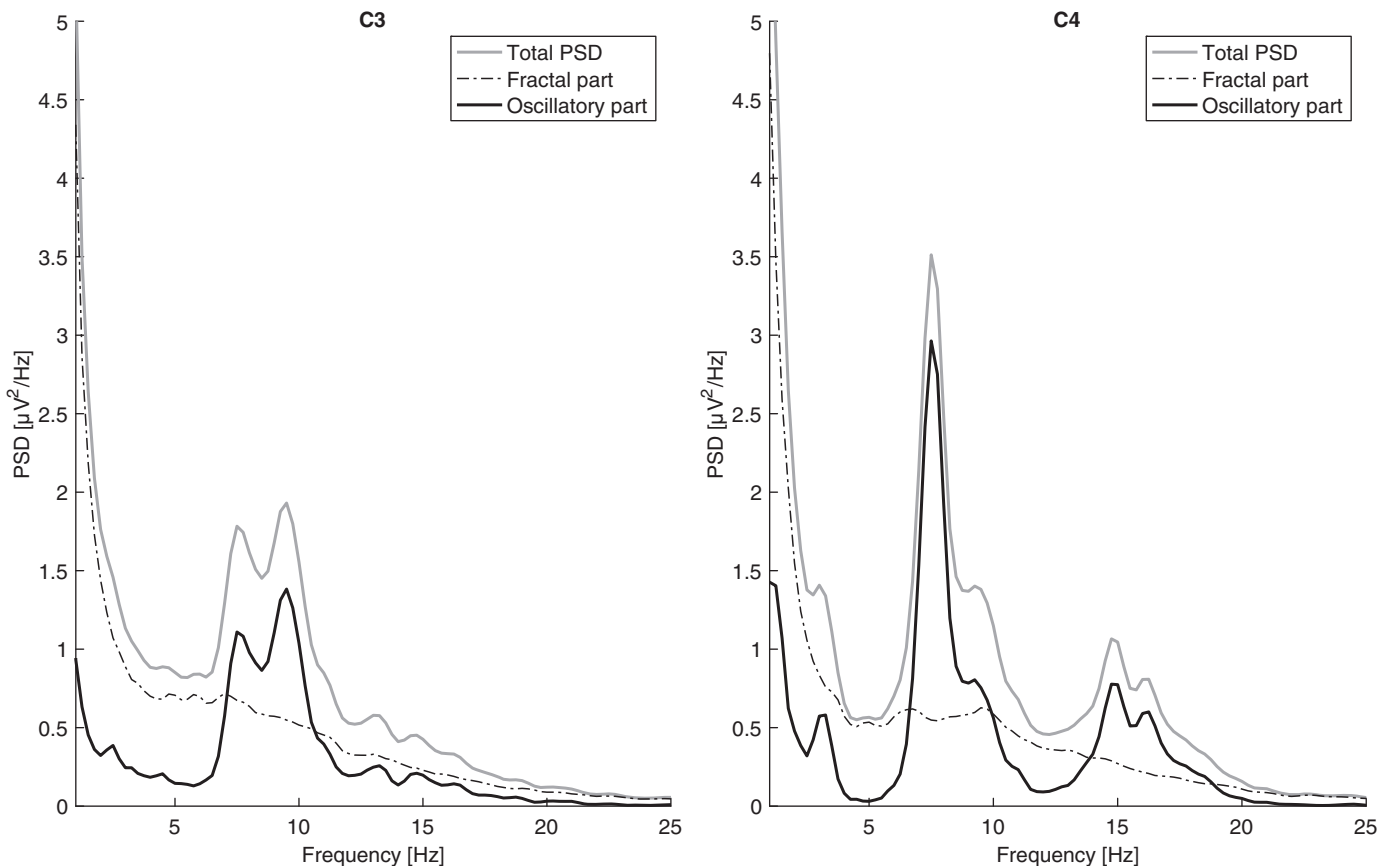

Fig. 3. Decomposition of the power spectrum density (PSD) into the fractal (scale-free) and oscillatory components underlying the eyes-closed awake state recorded after mirror-box training. Plots represent means of the irregular-resampling autospectral analysis (IRASA) decomposition computed separately for 4-s-long overlapping segments of approximately ~2-min-long resting block at two central EEG electrodes C3 and C4. Frequencies were restricted to the range 1–25 Hz for the visualization purposes.

$$\text{EEG response} = \beta_0 + \beta_1 \text{ date} + \varepsilon \qquad (1)$$

where β_0 is the model intercept, β_1 is an unknown regression coefficient (slope), and ε the model error. The model served to test the hypothesis $\beta_1 = 0$. If the hypothesis is rejected, a nonzero slope value is expected to reflect a longitudinal change of the EEG response over the whole experiment.

All tests employed a nominal two-sided 5% significance level ($\alpha = 0.05$). The Benjamini-Hochberg multiple comparisons procedure served to control the false discovery rate over all paired t-tests (Benjamini and Hochberg 1995).

RESULTS

We analyzed the EEG data collected from the hemiparetic patient during 51 mirror box training days over a period of 38 wk, with an average of 2 training days per week.

Detection of Oscillatory Rhythms

First, we analyzed the data from mirror box training blocks to determine major oscillatory rhythms associated with movements during the training. Using the proprietary APECSgui interface, we identified seven major PARAFAC atoms (components) for each training day, movement block, and spatial setting. We extracted the atoms separately for each of the two training blocks with the mirror box, i.e., the movement of the healthy hand only (VLH) and an attempt to move both hands (VBH), as well as separately by considering the whole set of 10 EEG electrodes placed over the sensorimotor area or 5 EEG electrodes placed either over the left or the right hemisphere.

The extracted atoms revealed a high stability and visual identifiability from day to day. Following the central peak frequency of the extracted PARAFAC frequency weight vectors and the visual inspection of the corresponding spectral weights averages, these atoms were denoted as: Theta (centered at 6 Hz), Mu (7.75 Hz), Alpha (9.25 Hz), SMR1 (11.5 Hz), SMR2 (13.5 Hz), Beta1 (16 Hz), and Beta2 (17.5 Hz). Note that this notation reflects specific narrow-band oscillatory rhythms we found for this subject and not the general EEG frequency ranges used in clinical studies. We used the term sensorimotor rhythm (SMR) for rhythms recorded over the sensorimotor cortical area and in the range 12–15 Hz (Sterman 1996). Further note that the extracted Alpha atom represents a posterior alpha rhythm with its maximal activation located in the parieto-occipital region and although the EEG channel O1 was not used in the PARAFAC model, this rhythm could still be detected from the more frontally placed EEG channels due to the volume conduction effects (Nunez and Srinivasan 2006). Although this rhythm is not in the focus of analyzing the movement-related oscillatory rhythms, it is included in the analysis to distinguish this rhythm from the sensorimotor Mu rhythm. Similarly, the Theta rhythm may not be directly linked to the movement process itself, but the time course of this rhythm may represent attentional or mental status related changes during the training.

Figure 4 depicts the mean values $\pm$ 1 SD of the PARAFAC frequency and spatial weights extracted from available records during the VLH training block and by considering the whole set of 10 sensorimotor EEG electrodes. PARAFAC results obtained
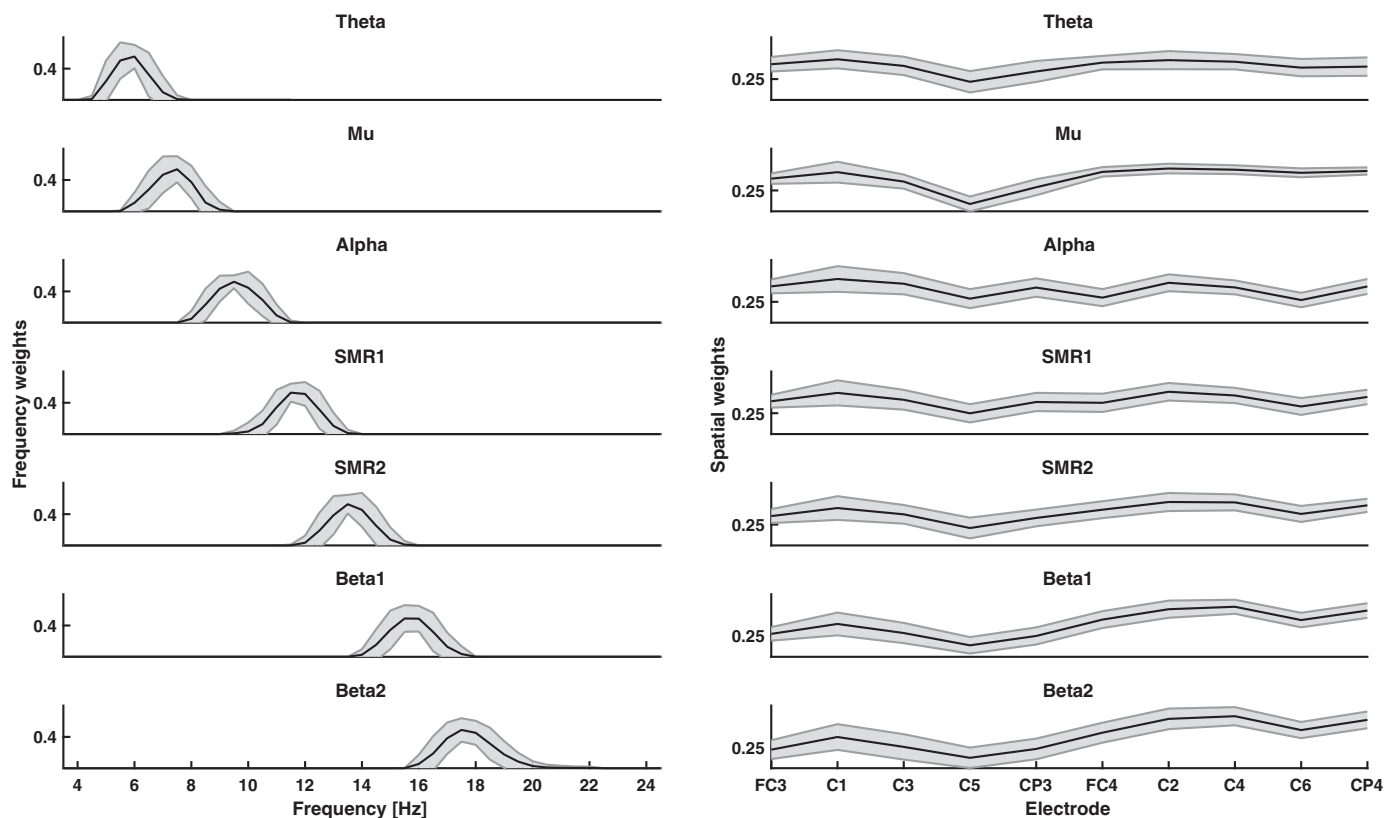

Fig. 4. Mean values of the parallel factor analysis (PARAFAC) frequency (*left*) and spatial (*right*) weight vectors obtained during the visual left hand training block (left-hand movement only) and by considering the whole set of 10 sensorimotor EEG electrodes. Each row represents the mean for one of the 7 extracted oscillatory rhythms (atoms). Values are averaged over all available records (days). Upper and lower limits of the shaded area represent the mean values $\pm$ 1 SD.

Fig. 5. Averaged harmonic part of the EEG power spectrum for the pretraining (black line) and posttraining (gray line) resting eyes-closed block. The values are averaged over all available records (days) and for each of the 11 EEG electrodes used.
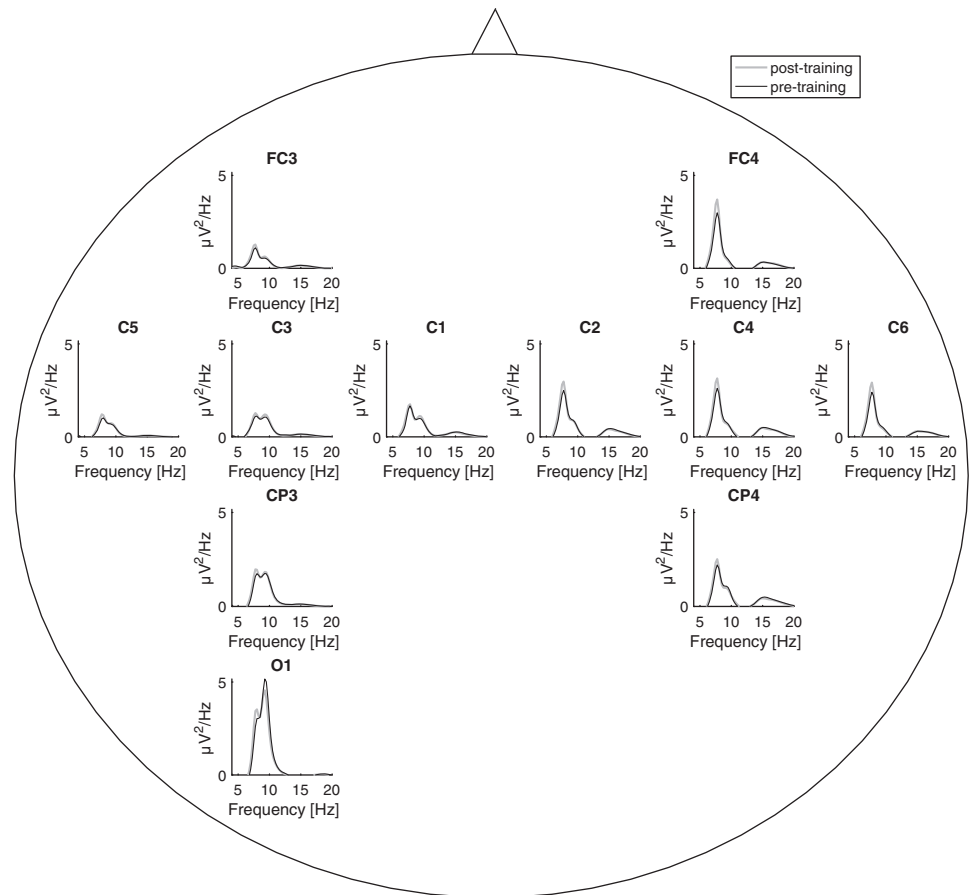
by using different model settings, either the VBH training block or the left and right electrodes only, resulted in the extraction of the same set of atoms. By considering both training conditions (VBH and VLH), and for each condition the three spatial settings of the EEG electrodes locations (all left and right electrodes or left or right hemisphere electrodes only), a very high stability represented by the low variance of the extracted PARAFAC frequency and spatial weight vectors was observed.

Analysis of Short-Term Effects

Next, we compared the averaged harmonic (oscillatory) part of the EEG power spectrum from the pre- and posttraining resting periods. We obtained the harmonic part by subtracting the fractal part of the spectrum from the raw power spectrum estimated with the IRASA method from the 4-s-long EEG segments, separately for each EEG electrode as well as for both EC and EO conditions. Due to the EEG artifacts, the number of days used to compute averages varied between electrodes but was in the range of 43–49 days for the EC and 48–51 days for the EO condition. In addition, we computed the difference between the post- and pretraining averaged harmonic power spectra. Figures 5, 6, 7, and 8 depict these harmonic averages as well as the differences.

Visual inspection. Visual inspection of these plots indicated a posttraining increase of the Mu rhythm power spectrum (centered at 7.75 Hz) during both EO and EC conditions, as well as an increase of the harmonic power spectrum in the range of SMR2 and Beta1 during the EO condition. Inspection of Theta (6 Hz) and posterior Alpha (9.5 Hz) rhythms indicated

the following changes: *1*) although no clearly visible change could be seen for theta (6 Hz) during the EC condition, for EO condition the differences at FC3, C3, and C1 channels (Fig. 8) indicated the theta-rhythm power increase; and *2*) alpha power decreased at O1 during EC and increased mainly in the left hemisphere during the EO condition.

Statistical testing. To test the statistical significance of these visually observed changes, we performed the following two analyses: first, we used paired *t*-tests to test the hypothesis of no difference between post- and pretraining resting block mean values of the harmonic part of the power spectrum around the central frequency of each of the seven identified oscillatory rhythms. To compensate for a small central peak frequency variation, we used the mean value of the harmonic power spectrum in the range of ±0.5 Hz around the central frequency.[1] We tested all available pre- and posttraining pairs from all days, separately for the EC and EO conditions.

Second, we used paired *t*-tests to test the hypothesis of no difference between post- and pretraining resting block mean time score values of the PARAFAC model. By projecting EO and EC EEG data to the extracted spatial and frequency weight vectors of the PARAFAC model, the time score vectors could be obtained. These time scores comprise spatial information from all electrodes used in the model, and for a given EEG segment and the activation of a given atom, we compute a single time score. Separately

---

[1] Note that with the sampling frequency of 128 Hz and the segment length of 4 s, the power spectrum is estimated with the 0.25-Hz frequency resolution, and therefore, every mean value is computed using five harmonic power spectrum values.
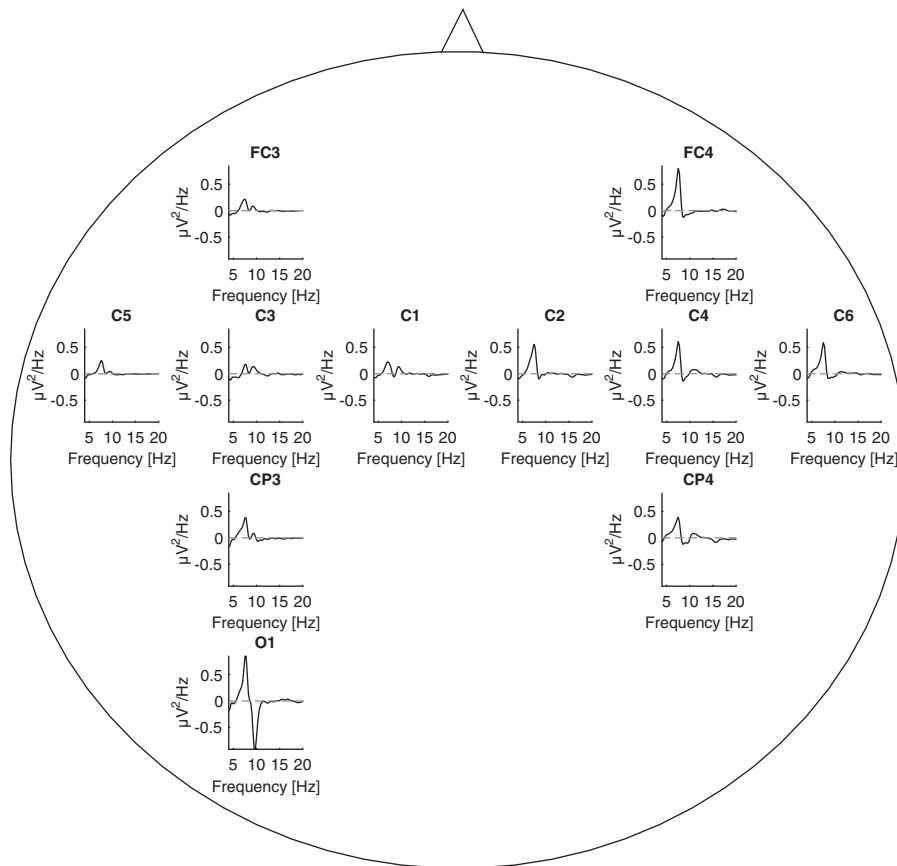
Fig. 6. Difference between posttraining and pretraining averaged harmonic parts of the EEG power spectrum depicted in Fig. 5.

Fig. 7. Averaged harmonic part of the EEG power spectrum for the pretraining (black line) and posttraining (gray line) resting eyes-open block. The values are averaged over all available records (days) and for each of the 11 EEG electrodes used.
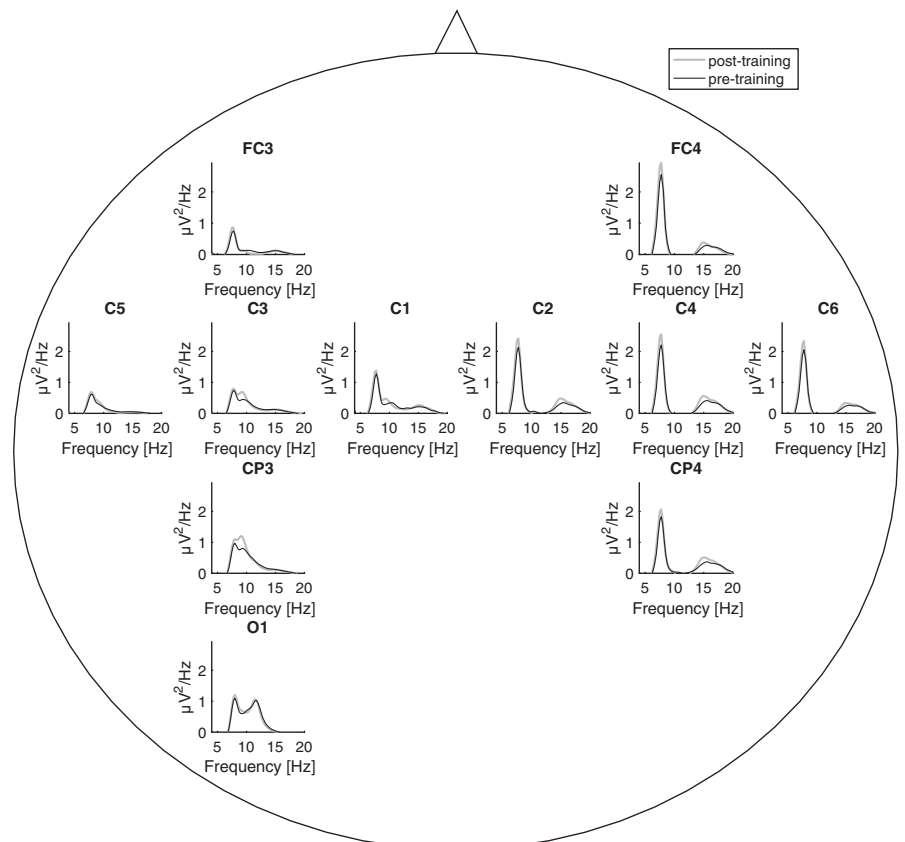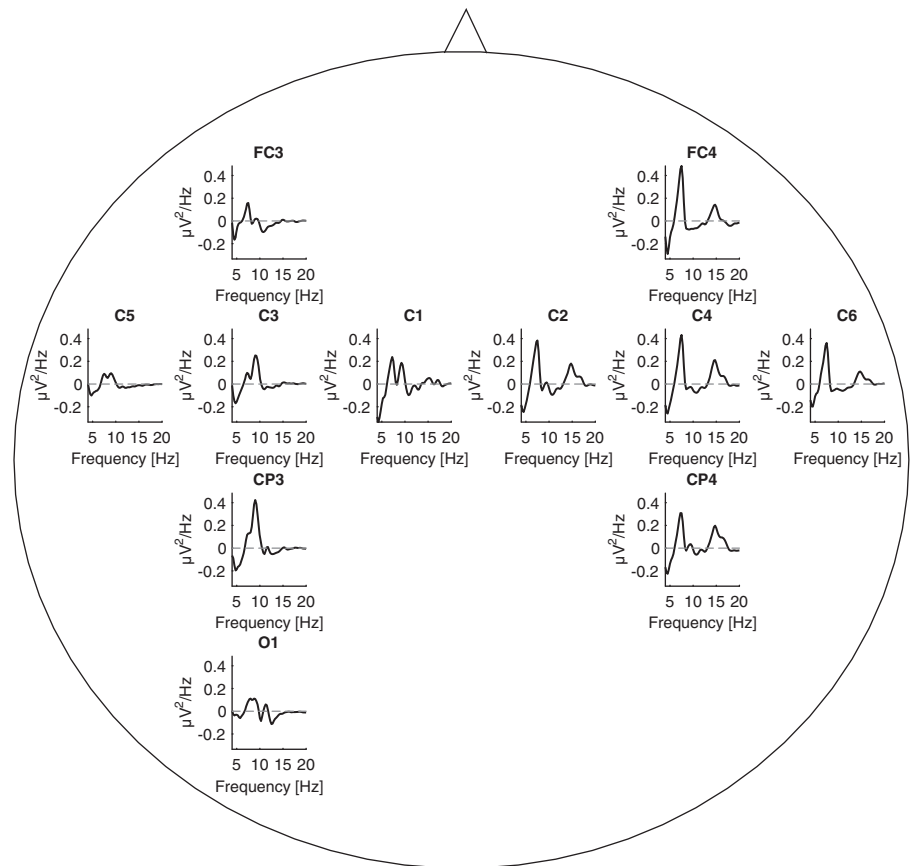
Fig. 8. Difference between posttraining and pretraining averaged harmonic parts of the EEG power spectrum depicted in Fig. 7.

for each pretest and posttest recording block and separately for the EC and EO conditions, we computed the mean time score value over the whole block by averaging the time scores computed for each 2-s long artifact-free EEG segment within each block. We used the data from all available mirror box training days. We performed the paired *t*-tests separately for each of the six considered PARAFAC models (factors VBH, VLH by left and right electrodes, left electrodes only, and right electrodes only), as well as separately for the EC and EO condition. Table 1 summarizes obtained *P* values of the paired *t*-tests.

Mu rhythm. Comparing the two testing approaches we can see a significant posttraining power increase of the Mu rhythm over the whole left and right sensorimotor region. This is true for both EC and EO conditions. This is a very consistent finding seen in both harmonic power spectrum representation as well as in the PARAFAC mean time scores approach.

SMR1, SMR2, Beta1, and Beta2 rhythms. We observed systematic power increases of the SMR2 and Beta1 rhythms in the right hemisphere during the EO condition. The PARAFAC time score representation also indicates an increase time scores of Beta2 in the left hemisphere. This contrasts with the EC condition, where both testing representations indicate a decrease of time scores of Beta1 and also Beta2 posttraining in the left hemisphere. For SMR1, no systematic change was observed for the EO condition. For the EC condition, we observed a significant increase in the harmonic power representation of this rhythm only in the area around the C2 electrode, but this was not consistent with the changes of the PARAFAC time scores.

Theta and Alpha rhythms. Theta, a rhythm not clearly related to movement, showed a consistent power increase at both

hemispheres for the EO condition. Results for the EC condition are less clear. The PARAFAC time scores did not confirm the observed power increase of Theta in the right hemisphere for the harmonic power spectrum. Posterior Alpha rhythm did not change at the occipital site O1. This was true for both the EO and EC conditions. Interestingly, we saw a posttraining power increase of this rhythm in the left hemisphere for the EO condition. There was no significant change in spectral power or time scores for Alpha in the EC condition.

Analysis of Long-Term Effects

Statistical testing. We tested the longitudinal effects of the mirror box training using the linear regression model (*Eq. 1*). The harmonic power spectrum served to represent the EEG response as a function of date. We computed the mean of the harmonic power spectrum over a single resting block and a day and representing one sample in the model. We fitted the models separately for each pre- and posttraining resting block, each of the seven oscillatory rhythms, each electrode, and each EC and EO condition. In addition, we also modeled the difference between the post- and pretraining harmonic power spectra as a function of test days. Again, we separately modeled EC and EO conditions and each rhythm and electrode. Finally, we also modeled the difference between the means of the post- and pretraining time scores representation of the six PARAFAC models as functions of test days.

Increases or decreases over test days are significant when the estimated β_1-regression coefficient (slope) is significantly nonzero after testing (*t*-statistic with $\alpha = 0.05$), that is, a signifi-

Table 1. *Significant P values of the paired t-test applied to test the difference between post- and pretraining mean values, in two resting conditions (EC and EO)*

	Theta 6 Hz	Mu 7.75 Hz	SMR1 11.5 Hz	SMR2 13.5 Hz	Beta1 16 Hz	Beta2 17.5 Hz	Alpha 9.25 Hz
EC							
FC3		0.0079					
C1	0.003				*0.0169*		
C3		0.0028					
C5		<0.0001			*0.0040*	*0.0060*	
CP3		0.0001					
O1	0.0073	<0.0001					
FC4	<0.0001	<0.0001					
C2	0.0005	0.0006			*0.0131*		
C4	0.0012	0.0003	0.0002				
C6	0.0001	<0.0001	0.0215				
CP4		0.0114	0.0173		*0.0041*		
VBH L		<0.0001		*0.0226*	*0.0031*	*0.0016*	
VBH R		<0.0001					
VBH LR		<0.0001				*0.0228*	
VLH L		<0.0001			*0.0030*	*0.0115*	
VLH R		<0.0001					
VLH LR		<0.0001					
EO							
FC3	0.0023	0.0007	*0.0002*				
C1	0.0001	0.0054			0.0002	0.0010	<0.0001
C3	0.0172	0.0070					<0.0001
C5		0.0031	*0.018*				<0.0001
CP3		0.0043		0.0075			<0.0001
O1				<0.0001			
FC4	<0.0001	0.0001		<0.0001		*0.0126*	*0.0198*
C2	<0.0001	0.0003		<0.0001	<0.0001		
C4	0.0121	0.0001		<0.0001	0.0001		
C6	0.0001	0.0005	*0.0075*	0.0135	0.0002		*0.0031*
CP4		0.0014		0.0002	<0.0001		*0.0063*
VBH L	<0.0001	<0.0001			0.0006	0.0003	<0.0001
VBH R	0.0002	<0.0001		0.0004	<0.0001		0.0173
VBH LR	<0.0001	<0.0001		0.0028	<0.0001	0.0007	<0.0001
VLH L	<0.0001	<0.0001			0.0006	0.0004	<0.0001
VLH R	<0.0001	<0.0001		0.0001	<0.0001		0.0091
VLH LR	<0.0001	<0.0001		0.0011	<0.0001	0.0002	<0.0001

Values in italic represent the mean value decrease at posttraining. The Benjamini-Hochberg multiple comparisons procedure for controlling the false discovery rate was applied. This led to the adjusted significance value $\alpha = 0.0257$. Table cells with dash represent cases where P values were greater than α. For eyes open (EO): significant P values for the harmonic power spectrum testing for 7 oscillatory rhythms at 11 EEG electrodes. Central frequency of each rhythm is defined in the *2nd row*. The mean harmonic power spectrum value of ± 0.5 Hz around each central frequency was used. For eyes closed (EC): significant P values for the parallel factor analysis (PARAFAC) mean time score values testing. VLH, movement of the healthy hand only; VBH, attempt to move both hands; L, left EEG electrodes; R, right EEG electrodes.

cant trend. Reported P values indicate the significance of this test.

Mu rhythm. The most consistent results were observed for the Mu rhythm. For the EC condition and the pretraining block, there was a significant increase in power (significant linear trend) over the period of 38 wk in both left and right hemispheres (Fig. 9). There was no significant change for the posttraining block. There was a significant decrease in the difference between post- and pretraining block power values in both hemispheres. The change of the post- and pretraining time score difference values showed a significant increase in the left hemisphere for both VBH L ($P = 0.018$) and VLH L ($P = 0.019$) PARAFAC models. Together with the paired *t*-test results (Table 1), this finding indicates the patient's Mu rhythm long-term power increased over the months of training. The observed long-term power increase at the pretraining block may account for the observed long-term decrease of the pre- and posttraining differences in power and PARAFAC time scores.

The results for the EO condition indicate a slightly different pattern. Analysis of the pretraining data shows that across the intervention period the Mu rhythm power increased in the right hemisphere. In the left hemisphere, power increased only at the C1 electrode ($P = 0.033$). In contrast to the EC condition, power increased for the posttraining block in both hemispheres. Considering the post- and pretraining difference, power increased only at the FC3 electrode ($P = 0.011$). This single significant difference is supported by a significant pre- and posttraining difference of the PARAFAC time scores in the left hemisphere; VBH L ($P = 0.002$) and VLH L ($P = 0.010$). Again, together with the paired *t*-test (Table 1), this finding indicates a long-term power increase of the Mu rhythm predominantly in the right hemisphere. There were also increases of the differences in pre- and posttraining block power and PARAFAC time score difference values in the left hemisphere.

SMR1, SMR2, Beta1, and Beta2 rhythms. Analyzing the other four movement-related oscillatory rhythms (SMR1, SMR2, Beta1, and Beta2), we observed a significant increase of the posttraining SMR1 and SMR2 harmonic power spectrum at the CP3 electrode. This was true for both EC and EO ($P < 0.023$). However, there were no significant trends for the
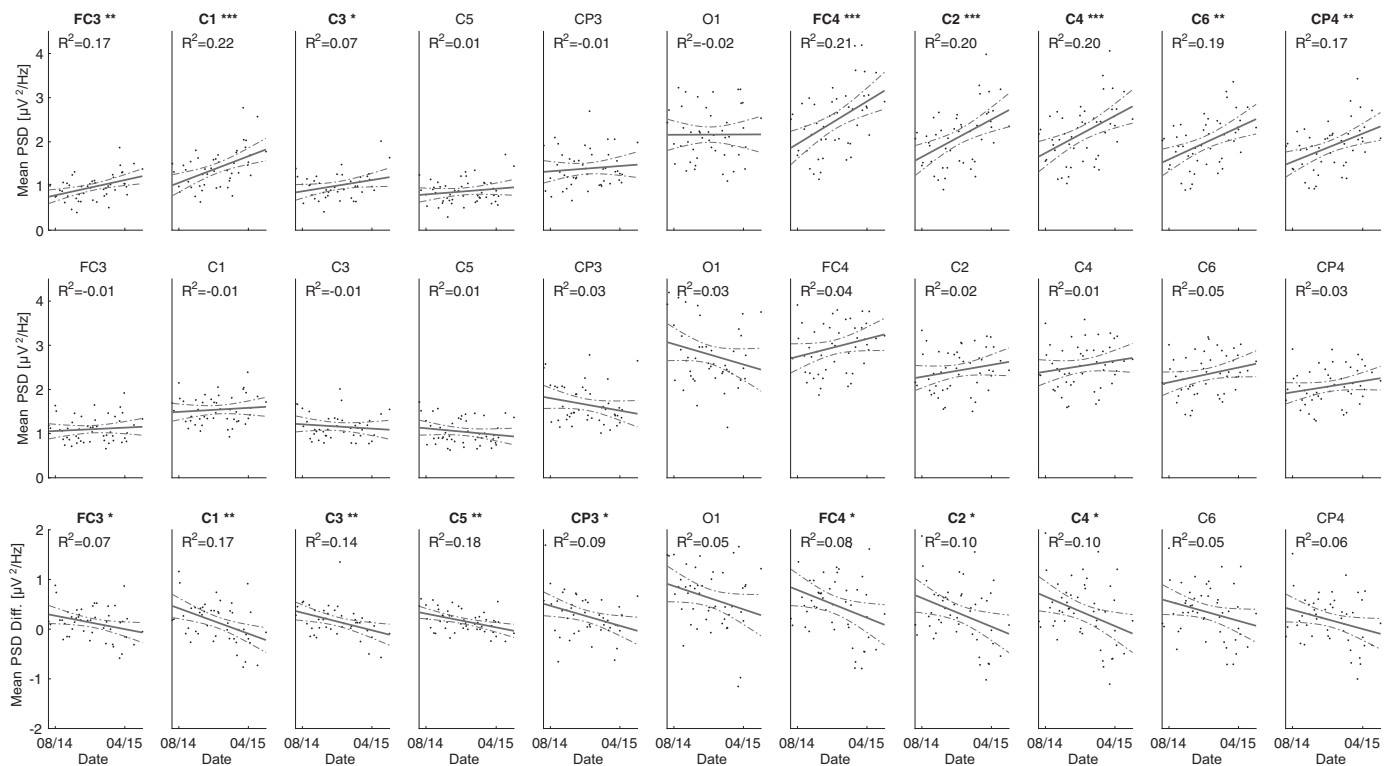
Fig. 9. Averaged Mu rhythm harmonic part of the EEG power spectrum for the eyes-closed condition. Each value is an average computed for a session (day). The time period from July 2014 until April 2015 is depicted. *Rows 1* and *2*: averages of pretraining and posttraining periods. *Row 3*: post- and pretraining difference. Solid lines represent a linear fit to data, and 95% confidence interval for each point is represented by dashed-dotted lines. Adjusted coefficient of determination R^2 is displayed at the *top* of each subplot. *$P < 0.05$, **$P < 0.01$, ***$P < 0.001$, linear fits with significant nonzero slopes.

pretraining block and the pre- and posttraining block differences. As for SMR, there was a posttraining power increase of Beta1 at CP3 ($P = 0.002$), but only for the EO condition; however, in contrast to SMR, there was also a significant power increase in the post- and pretraining difference ($P = 0.005$). The difference between post- and pretraining PARAFAC time scores was significant for VBH L ($P = 0.009$) and VLH L ($P = 0.008$), supporting the results of the harmonic power spectrum representation. In contrast, power decreased for Beta2. The pretraining power decrease was significant at C3 ($P < 0.040$) and C5 ($P < 0.022$) for both EC and EO conditions and at C6 ($P = 0.013$) for the EO condition. A decrease in posttraining power occurred for the EO condition at C4 ($P = 0.035$). The pre- and posttraining power difference increased for EO at C5 ($P = 0.003$) and CP3 ($P = 0.015$) and for VBH L ($P = 0.003$) and VLH L ($P = 0.009$) time scores. For the EC condition, the increase of pre- and posttraining power differences was significant at C5 ($P = 0.005$).

In summary, the observed power changes of SMR1, SMR2, Beta1, and Beta2 were less consistent than those for the Mu rhythm and were observed only at a few central and centroparietal electrodes, mainly in the left hemisphere. The results suggest that for SMR1, SMR2, and Beta1, the observed increasing power in the left hemisphere is short term and due to the training itself, while the observed left hemisphere Beta2 decreasing power may reflect a longer term effect of the mirror box training.

Theta and Alpha rhythms. The analysis of Theta and Alpha rhythms revealed consistent changes for Theta only. There were

significant power increases of Theta during the posttraining EC block at several left (C1, C3, and C5) and right (FC4, C2, and CP4) hemisphere electrodes ($P < 0.046$). Pretraining power increased at C1 ($P = 0.024$) and FC4 ($P = 0.026$). No significant changes occurred for the post- and pretraining difference. For the EO condition, we saw a similar pattern for the post- and pretraining blocks. Specifically, posttraining Theta power increased at left (FC3 and C1) and right (FC4, C4, and C6) electrodes ($P < 0.043$) and pretraining power increased at FC4 only. However, in contrast to the EC condition, significant changes of the post- and pretraining difference values occurred for the harmonic power spectrum at FC3, C5, Cp3, and FC4 ($P < 0.038$). Post- and pretraining difference in time scores confirmed this finding ($P < 0.011$) in all six PARAFAC models. Together with the paired *t*-test (Table 1), these results indicate a significant effect of training on increasing power of the Theta rhythm in both left and right hemispheres. However, the effect seems to be short term only and stronger for the EO condition than for EC.

Finally, Alpha posttraining power and pre- and posttraining power differences increased, but only at a single electrode CP4 ($P = 0.04$), and only for the EO condition. Therefore, we do not consider this effect stable and consistent.

Clinical Evaluation

Quantitative evaluation of clinical movement testing during the study is summarized in Fig. 10. Figure 10, *top*, shows a very mild increase (with respect to the ranges) of FMA and MSIS scores for upper extremity. The spasticity of the upper extremity was surprisingly released as reflected in MAS. Figure 10, *middle* and *bottom*, reveals a mild improvement (with respect to the overall
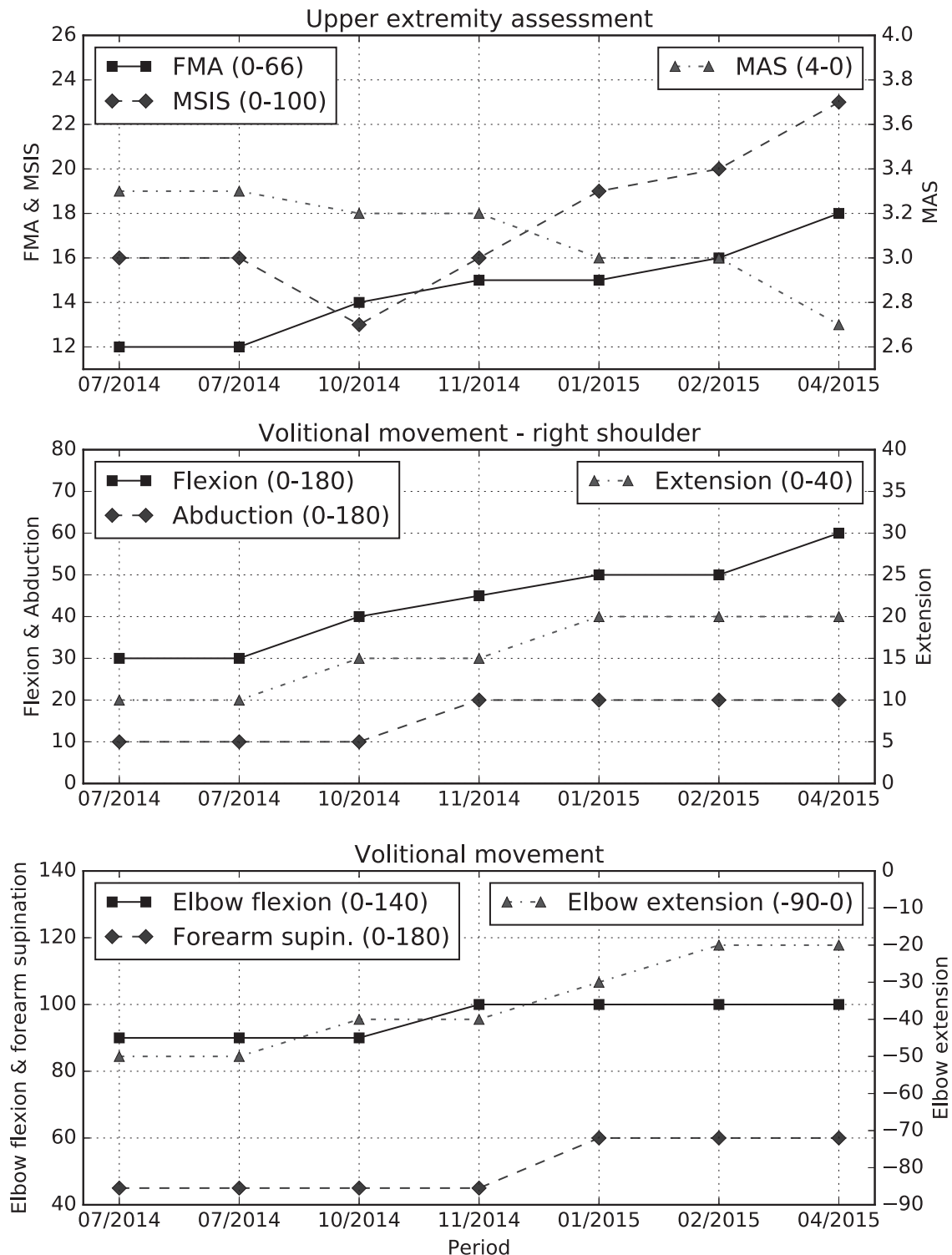
Fig. 10. Changes in various measures during the course of the longitudinal study. *Top:* upper extremity assessment: Fugl-Meyer Assessment (FMA) and Modified Stroke Impact (MSIS) scale both increase but very slightly with respect to the overall ranges. The spasticity of the upper extermity is surprisingly released as reflected in and Modified Ashworth Scale (MAS). The ranges of these 3 scales are in brackets, where higher values of FMA and MSIS indicate better movement ability, while this is reflected by smaller values of MAS. *Middle:* volitional movement of the right arm: Arm flexion and arm abduction increase but very slightly with respect to the overall ranges. Arm extension increases more evidently with respect to the overall range. *Bottom:* volitional movement of the right elbow and forearm during the course of the longitudinal study: elbow extension, elbow flexion, and forearm supination all increase, but very slightly with respect to the overall ranges.

range) of an active movement of the right arm, elbow, and forearm. However, the wrist and fingers remained plegic, and hence, the motor assessment scale of the hand did not show any progress (not plotted).

DISCUSSION

To our knowledge, this is the first longitudinal study of MT effects on modulation of EEG oscillatory rhythms. Resting state EEG recorded pre- and postmirror box training served to

investigate short-term effects as well as to detect longer term effects lasting from day-to-day and spanning over the whole period of the experiment.

The focus of the study was on oscillatory EEG rhythms associated with movement. It is important to stress that identification of central peak frequencies of these rhythms has to be carefully done by including spatial and experimental condition information. We argue, that even when considering a larger cohort of subjects, this needs to be carried out for each subject individually. Considering the standard clinical EEG frequency bands is not adequate, because these bands are not specific to individuals, are too wide, and can mix several oscillatory sources at a given spatial location mainly due to the volume conduction effect on EEG (Nunez and Srinivasan 2006). Application of the fractal and harmonic decomposition of the EEG spectrum, as well as the identification of frequency and spectral PARAFAC loadings of the main oscillatory sources, represents efficient methods addressing this problem (Rosipal et al. 2009; Wen and Liu 2016). Using this approach, we reliably identified five oscillatory rhythms related to passive movement watching or active movement.

Among these five rhythms, the most consistent and significant mirror box training effect occurred for the Mu rhythm. When the Mu rhythm was analyzed, the harmonic power spectrum observed in the left hemisphere, the hemisphere affected by stroke, was smaller by about a factor of two in comparison to the right hemisphere. Note that the MRI scan revealed ischemia extending from the fronto-temporal to parietal areas on the left side. In contrast to the posterior Alpha rhythm, the Mu rhythm is not blocked by closing the eyes (Pineda 2005). This was confirmed in our study, however, a decrease of ~0.3 to 0.4 μV^2/Hz was observed when comparing EO and EC harmonic power averages.

We found significant changes of the Mu rhythm power for both the pre- and posttraining differences and long-term increasing trends. This is an important result of the study, which indicates that the long-term mirror box training increases the resting state Mu rhythm in both left and right sensorimotor areas and this is true for both resting conditions: EO and EC.

When the other four rhythms were analyzed, the training effects were not as clear as in the case of the Mu rhythm. The mirror box training increased SMR1, SMR2, and Beta1 mainly in the left, affected hemisphere, but the effect was only short term, i.e., session based. In contrast, a decrease of Beta2 as a longer term effect of the mirror box training was observed in the same hemisphere.

Although the posterior Alpha rhythm changes during the resting, movement observation and movement periods of the mirror box training, no significant changes were observed when the pre- and posttraining resting state EEG data were analyzed.

For the Theta rhythm, we found short-term increases in both band power and PARAFAC time scores. This was true for both hemispheres, and the change was stronger for the EO condition than for EC. During the EO condition, we also observed a short-term increase in power of the posterior Alpha rhythm in the central and centro-parietal regions of the left hemisphere. One explanation could follow our previous findings that these increases in Theta and Alpha are related to increased mental fatigue of the patient during the training sessions (Trejo et al. 2015). This is also supported by our subjective observation

where mental exhaustion of the patient, especially after his attempts to move his hemiparetic arm during the VBH block, was clearly observable at many sessions.

We are not aware of any prior study focusing on the effects of MT on the power spectrum of narrow-band, movement-related, EEG oscillatory rhythms. However, there is an extensive literature within the brain computer interface (BCI) community showing the effect of motor imagery training on motor recovery and changes of motor-related EEG rhythms (e.g., Pichiorri et al. 2015). BCI training consists of instrumental conditioning or rewarding of expected ERS and ERD changes modulated by the subject's mental imagery of movement. While rewarding in the BCI protocols may play its role, there is growing evidence that a link between motor imagery and passive action observation exists (Case et al. 2015; de Vries and Mulder 2007; Mulder 2007). Our results are in the line with these findings, indicating that changes in the activation (ERD) and deactivation (ERS) of motor cortical regions during MT leads to the power spectrum changes of motor-related oscillatory rhythms detected in the scalp EEG. Moreover, we designed and tested a BCI-based robotic system (robotic splint) using the motor imagery paradigm. After MT, the patient participated in this follow-up training, where the same identified Mu rhythm was used to control the splint through the process of ERS/ERD induced by motor imagery. Time scores of this rhythm were used to trigger the splint. The results of this BCI training are not part of this paper, but they resemble reported findings (Rosipal et al. 2018).

Although the focus of the study was on objective electrophysiological changes of the brain response to MT, we also performed a clinical evaluation of the subject's upper limb movement abilities. The clinical tests indicate a slight improvement in movement and spasticity of the arm but without a detectable progress for wrist and fingers. It is worth noting that the subject entered the study as late as 2 yr after stroke with a severely plegic hand. Subjectively, we observed an improvement in subject's speech and social communication; however, this was not clinically tested. The subject showed strong enthusiasm to participate.

Finally, note that although this is a single case study, it is used as demonstration, not as a population-based statistical proof. However, it needs to be also realized that to set and carry out well designed control study focused on significant group effects would be difficult and costly. It would require to recruit stroke patients with a comparable lesion and functional impairments and to consider randomized grouping into a different type or no intervention. Willingness of patients to participate for such a long period of time would also be an issue. On the other hand, large interindividual differences in EEG oscillatory rhythms and their detection, as well as a wide spectrum of clinical, stroke severity, and movement impairment aspects may require an individualized approach when the effects of MT on EEG oscillatory changes are studied. On the other hand, and in our opinion, in the clinic it does not really matter how many responders to a given therapy we have: it is valuable if it may work for some.

Finally, without a doubt, EEG is becoming a standard diagnostic tool in clinic and the design of our experiment can be easily replicated, so we believe that we may see more outcomes in the direction of our research in the near future.

REFERENCES

Andersson CA, Bro R. The N-way toolbox for MATLAB. *Chemom Intell Lab Syst* 52: 1–4, 2000. doi:10.1016/S0169-7439(00)00071-X.

Bähr F, Ritter A, Seidel G, Puta C, Gabriel HH, Hamzei F. Boosting the motor outcome of the untrained hand by action observation: mirror visual feedback, video therapy, or both combined-what is more effective? *Neural Plast* 2018: 8369262, 2018. doi:10.1155/2018/8369262.

Benjamini Y, Hochberg Y. Controlling the false discovery rate: a practical and powerful approach to multiple testing. *J R Stat Soc B* 57: 289–300, 1995.

Bro R. PARAFAC: Tutorial and applications. *Chemom Intell Lab Syst* 38: 149–171, 1997. doi:10.1016/S0169-7439(97)00032-4.

Case LK, Pineda J, Ramachandran VS. Common coding and dynamic interactions between observed, imagined, and experienced motor and somatosensory activity. *Neuropsychologia* 79: 233–245, 2015. doi:10.1016/j.neuropsychologia.2015.04.005.

Chaudhary U, Birbaumer N, Ramos-Murguialday A. Brain-computer interfaces for communication and rehabilitation. *Nat Rev Neurol* 12: 513–525, 2016. doi:10.1038/nrneurol.2016.113.

de Vries S, Mulder T. Motor imagery and stroke rehabilitation: a critical discussion. *J Rehabil Med* 39: 5–13, 2007. doi:10.2340/16501977-0020.

Doppelmayr M, Klimesch W, Pachinger T, Ripper B. Individual differences in brain dynamics: important implications for the calculation of event-related band power. *Biol Cybern* 79: 49–57, 1998. doi:10.1007/s004220050457.

Garry MI, Loftus A, Summers JJ. Mirror, mirror on the wall: viewing a mirror reflection of unilateral hand movements facilitates ipsilateral M1 excitability. *Exp Brain Res* 163: 118–122, 2005. doi:10.1007/s00221-005-2226-9.

Gurbuz N, Afsar SI, Ayaş S, Cosar SNS. Effect of mirror therapy on upper extremity motor function in stroke patients: a randomized controlled trial. *J Phys Ther Sci* 28: 2501–2506, 2016. doi:10.1589/jpts.28.2501.

He BJ. Scale-free brain activity: past, present, and future. *Trends Cogn Sci* 18: 480–487, 2014. doi:10.1016/j.tics.2014.04.003.

Jones L, van Wijck F, Greally M, Rowe P. A changing stroke rehabilitation environment: implications for upper limb interventions. *5th IEEE International Conference on Pervasive Computing Technologies of Healthcare (Pervasive Health)*, Dublin, Ireland, May 23–26, 2011, p. 374–378.

Klimesch W. Memory processes, brain oscillations and EEG synchronization. *Int J Psychophysiol* 24: 61–100, 1996. doi:10.1016/S0167-8760(96)00057-8.

Lim KB, Lee HJ, Yoo J, Yun HJ, Hwang HJ. Efficacy of mirror therapy containing functional tasks in poststroke patients. *Ann Rehabil Med* 40: 629–636, 2016. doi:10.5535/arm.2016.40.4.629.

Mareček R, Lamoš M, Labounek R, Bartoň M, Slavíček T, Mikl M, Rektor I, Brázdil M. Multiway array decomposition of EEG spectrum: implications of its stability for the exploration of large-scale brain networks. *Neural Comput* 29: 968–989, 2017. doi:10.1162/NECO_a_00933.

Miwakeichi F, Martínez-Montes E, Valdés-Sosa PA, Nishiyama N, Mizuhara H, Yamaguchi Y. Decomposing EEG data into space-time-frequency components using parallel factor analysis. *Neuroimage* 22: 1035–1045, 2004. doi:10.1016/j.neuroimage.2004.03.039.

Mulder T. Motor imagery and action observation: cognitive tools for rehabilitation. *J Neural Transm (Vienna)* 114: 1265–1278, 2007. doi:10.1007/s00702-007-0763-z.

Nunez PL, Srinivasan R. *Electric Fields of the Brain: The Neurophysics of EEG*. New York: Oxford University Press, 2006. doi:10.1093/acprof:oso/9780195050387.001.0001.

Oberman LM, Pineda JA, Ramachandran VS. The human mirror neuron system: a link between action observation and social skills. *Soc Cogn Affect Neurosci* 2: 62–66, 2007. doi:10.1093/scan/nsl022.

Pacific Development and Technology. *APECSgui. Installation Guide and User Manual, Version 1.0* (Online). https://www.pacdel.com/upload/files/pdt-apecsgui-software-manual.pdf [31 March 2012].

Pangman VC, Sloan J, Guse L. An examination of psychometric properties of the mini-mental state examination and the standardized mini-mental state examination: implications for clinical practice. *Appl Nurs Res* 13: 209–213, 2000. doi:10.1053/apnr.2000.9231.

Pérez-Cruzado D, Merchán-Baeza JA, González-Sánchez M, Cuesta-Vargas AI. Systematic review of mirror therapy compared with conventional rehabilitation in upper extremity function in stroke survivors. *Aust Occup Ther J* 64: 91–112, 2017. doi:10.1111/1440-1630.12342.

Pfurtscheller G, Lopes da Silva FH. Event-related EEG/MEG synchronization and desynchronization: basic principles. *Clin Neurophysiol* 110: 1842–1857, 1999. doi:10.1016/S1388-2457(99)00141-8.

Pichiorri F, Morone G, Petti M, Toppi J, Pisotta I, Molinari M, Paolucci S, Inghilleri M, Astolfi L, Cincotti F, Mattia D. Brain-computer interface boosts motor imagery practice during stroke recovery. *Ann Neurol* 77: 851–865, 2015. doi:10.1002/ana.24390.

Pineda JA. The functional significance of mu rhythms: translating "seeing" and "hearing" into "doing". *Brain Res Brain Res Rev* 50: 57–68, 2005. doi:10.1016/j.brainresrev.2005.04.005.

Rizzolatti G, Craighero L. The mirror-neuron system. *Annu Rev Neurosci* 27: 169–192, 2004. doi:10.1146/annurev.neuro.27.070203.144230.

Rosipal R, Porubcová N, Cimrová B, Farkaš I. Mirror-therapy as a way to start BCI robot-assisted rehabilitation: a single case longitudinal study of a patient with hemiparesis. In: *The Seventh International BCI Meeting, Pacific Grove, CA, May 21–25*. Poster available at http://aiolos.um.savba.sk/~roman/Papers/bci18.pdf [2018].

Rosipal R, Trejo LJ, Nunez PL. Application of multi-way EEG decomposition for cognitive workload monitoring. In: *Proceedings of the 6th International Conference on PLS and Related Methods*, edited by Esposito Vinzi V, Tenenhaus M, Guan R. Beijing: Publishing House of Electronics Industry, 2009, p. 145–149.

Shimazu H, Maier MA, Cerri G, Kirkwood PA, Lemon RN. Macaque ventral premotor cortex exerts powerful facilitation of motor cortex outputs to upper limb motoneurons. *J Neurosci* 24: 1200–1211, 2004. doi:10.1523/JNEUROSCI.4731-03.2004.

Sterman MB. Physiological origins and functional correlates of EEG rhythmic activities: implications for self-regulation. *Biofeedback Self Regul* 21: 3–33, 1996. doi:10.1007/BF02214147.

Trejo LJ, Kubitz K, Rosipal R, Kochavi RL, Montgomery LD. EEG-based estimation and classification of mental fatigue. *Psychology (Irvine)* 6: 572–589, 2015. doi:10.4236/psych.2015.65055.

Trejo LJ, Rosipal R, Nunez PL. *Advanced Physiological Estimation of Cognitive Status (APECS). Final Project Report*. Research Triangle Park, NC: U.S. Army Research Office, 2009. doi:10.21236/ADA520986.

Wen H, Liu Z. Separating fractal and oscillatory components in the power spectrum of neurophysiological signal. *Brain Topogr* 29: 13–26, 2016. doi:10.1007/s10548-015-0448-0.